Atmospheric-pressure cold plasma: a friendly environment for dry enzymes

Fiorenza Fanelli, [†] Francesco Fracassi,[†,‡] Annamaria Lapenna,[‡] Valeria Angarano,[£] Gerardo Palazzo, [‡,$] Antonia Mallardi[§]

AUTHOR ADDRESS:
[†] CNR-NANOTEC National Research Council, Institute of Nanotechnology, c/o Department of Chemistry, University of Bari 'Aldo Moro', via Orabona 4, 70126 Bari, Italy
[‡]Department of Chemistry, University of Bari 'Aldo Moro', via Orabona 4, 70126 Bari, Italy
[§] CNR-IPCF, National Research Council, Institute for Chemical-Physical Processes, c/o Department of Chemistry, University of Bari 'Aldo Moro', via Orabona 4, 70126 Bari, Italy
[£] BioTeC+, Chemical and Biochemical Process Technology and Control Department of Chemical Engineering, KU Leuven, Gebroeders De Smetstraat 1, 9000 Ghent (Belgium)
[$] CSGI (Center for Colloid and Surface Science) c/o Dept. Chemistry, via Orabona 4, 70125 Bari, Italy

ABSTRACT:
A comprehensive study of the interaction of atmospheric pressure cold plasmas with dry enzymes was conducted to identify the experimental conditions that allow preserving enzyme functionality. Specifically, dry deposits of glucose oxidase (GOx) and tyrosinase (Tyr) were exposed to dielectric barrier discharges fed with pure helium, helium-oxygen and helium-ethylene mixtures, to reproduce the main plasma processes relevant to surface engineering, i.e., plasma treatment, plasma etching and plasma-enhanced chemical vapour deposition (PE-CVD), respectively. Results reveal that the plasma-enzyme interaction leads to considerable decrease of enzyme activity only in case of oxygen-containing feed mixtures, for relatively harsh conditions of applied voltage (1.1 kV_{rms}) and very long exposure time (> 30 min). The two enzymes respond differently to plasma exposure. GOx is more prone to etching in oxygen-containing DBDs, however the decrease in enzyme activity due to protein ablation can be reduced by increasing the thickness of the initial enzyme deposit. In contrast, Tyr suffers a certain inactivation upon plasma exposure, though showing strong etching resistance. Interestingly, the customary conditions used for PE-CVD using helium/ethylene mixtures (applied voltage < 1.1 kV_{rms} and exposure time ≤ 10 min) are friendly for both GOx and Tyr. It is therefore possible to immobilize enzymes by overcoating with a plasma-deposited thin film, fully retaining enzyme functionality. Overall, the results of the present study enlighten an unexpected high stability of dry enzymes upon plasma exposure and allow envisaging new directions towards surface engineering of enzymes through plasma-based approaches.

INTRODUCTION

The machinery of life is based on chains of several enzymes that catalyse in cascade a series of selective reactions in which the product of a reaction becomes the substrate of the following one. To work properly, the rates of all the processes (including the reaction and diffusion steps) must be finely tuned. This means that the different enzymes must be present at the optimal ratios and often in a given spatial arrangement.[1,23,4] In principle, such an approach could be implemented in many analytical, industrial and biotechnological applications, provided that enzymes are assembled in the desired mole ratios, according to suitable architectures and in a way that preserves their activity ensuring their recovery and re-use.[5] Actually, the state of affairs in multi-enzymes immobilization is yet embryonic because the traditional four methods used (physical adsorption, entrapment, covalent attachment, and bioaffinity)[6] do not allow a fine control of the loading of different enzymes. Furthermore, the additional time requirement and costs associated with the enzyme immobilization are often considerable so that only relatively few processes employing immobilized enzymes have been successfully commercialized.[7]

Recently, a new one-step immobilization procedure, based on non-equilibrium (cold) plasma processing, has been proposed. [8,9,10] Cold plasmas are neutral partially ionized gases which can be generated by applying a direct or alternating electrical field to a gas mixture using suitable plasma reactors. Since the nature of the feed gas and the experimental conditions (e.g., reactor design, electrical excitation parameters, pressure, feed gas flow rate) tune the density of the reactive plasma-generated species (i.e., atoms, radicals, ions, and electrons), different interactions between the plasma and the surfaces can take place, leading to three main processes:

i) *Dry etching*, where cold plasmas fed with proper reactive gases induce massive reactions between the plasma generated species and the material, forming volatile products and leading to true ablation.
ii) *Plasma-assisted deposition* of thin coatings (up to a few μm thickness), using different approaches such as the plasma-enhanced chemical vapor deposition (PE-CVD) which exploits feed mixtures containing at least one plasma-polymerizable gas acting as thin film precursor.
iii) *Plasma treatment*, when only the modification of the uppermost layers of the surface occurs, through for instance grafting of functional groups and/or variation of the cross-linking degree and of the surface roughness, without massive etching or thin film deposition.

Of course, depending on the experimental conditions, etching, treatment and thin film deposition can also co-exist.

All these plasma processes have been extensively used to modify solid surfaces in a way that permits, in a second step, the enzyme immobilization by wet physical adsorption, chemi- or bio-coniugation.[11,12] The recently proposed one-step strategy consists of injecting simultaneously a suitable organic coating precursor with an atomized enzyme solution directly in an atmospheric pressure cold plasma.[3,4,5] During the process, the plasma-activated precursor polymerizes and entraps the biomolecules in the growing thin film. Such an approach has the merit to be time-saving and could potentially be used for the deposition of several enzymes in a given ratio (e.g., by feeding the atomizer with a multi-enzyme solution). However, due to the single step nature of the procedure it is not possible to control the quantity of the enzyme deposited as well as the fraction of enzyme that retains its functionality. This lack of information does not allow the rational optimization of the process and hampers the development and utilization of multi-enzymes immobilizations.

The concerns about the enzyme inactivation are not hypothetical. Indeed, impressive results have been achieved exploiting atmospheric pressure cold plasmas for the inactivation of micro-organisms,[13] cells[14,15] and enzymes[16] in the fields of plasma medicine[17] and food processing.[18,19] Depending on the conditions, the interaction between plasma and proteins can be blasting (e.g., dry etching has been proposed as method to remove prions from surgical instruments)[20] or friendly (e.g., a biosensor containing functional enzymes overcoated through PE-CVD has been reported)[21]. Despite such a wide range of different implications, there is a lack of fundamental studies on the conditions that allow preserving or destroying the enzyme functionality. In the attempt to fill such a gap we have undertaken a systematic study of the effect of atmospheric pressure cold plasma on enzyme functionality, focusing the attention on the influence of the nature of the feed mixture, the plasma excitation conditions, the exposure time and the amount of the enzyme itself.

We have used two different enzymes as model systems: the glucose oxidase (GOx) and the tyrosinase (Tyr). The GOx is an oxygen-dependent glycoprotein and, being the biological key of the biosensors for diabetes monitoring, is one of the most studied immobilized enzyme[22]. Tyrosinase, on the other hand, is a copper-enzyme which in presence of oxygen catalyzes the first two steps in melanogenesis and is responsible for enzymatic browning reactions in foods[23,24]. Depending on the applications one can be interested in preserving the tyrosinase activity (as in the fabrication of biosensors for phenolic compounds) or in it deactivation (e.g. to avoid the browning of foods).
In this work, known amounts of enzymes have been deposited by drop casting onto a solid support and exposed after drying to atmospheric pressure cold plasmas generated using a parallel plate dielectric barrier discharge (DBD) reactor. As feed gas we have used either pure helium and helium-based mixtures (viz. helium-oxygen and helium-ethylene) in order to reproduce the main processes that take place when a plasma interacts with a surface, viz. plasma treatment, plasma etching, and plasma deposition, respectively. Note that in the case of plasma deposition, the final outcome is that of a dry enzyme deposit overcoated with a polymeric thin film (i.e., polyethylene-like coating).[25] This last process can be easily extended to mixtures of enzymes, thus representing a simple method to immobilize known amount of different enzymes.

RESULTS AND DISCUSSION

The main motivation of the present work is to find the conditions of PE-CVD using atmospheric pressure DBDs fed with a polymerizable gas that preserve the maximum enzyme functionality, thus permitting useful enzyme immobilization by overcoating. It is important to keep in mind that the proposed immobilization approach involves the direct exposure of dry enzymes to the atmospheric pressure cold plasma and, therefore, the plasma/enzyme interaction deserves a more extended investigation. To obtain a clearer picture of the different processes that can take place when an atmospheric pressure cold plasma interacts with dry enzymes, we investigated and optimized the experimental conditions of processes carried out using DBDs fed with:

i) pure helium (i.e., the DBD process main gas),[26] as representative of plasma treatment;
ii) helium/1% oxygen mixture, that could induce considerable enzyme etching;
iii) helium/ethylene mixtures under optimized conditions to obtain PE-CVD and overcoat the enzyme with a polyethylene-like thin film.

Glucose oxidase and tyrosinase were deposited on glass slides by drop-casting (5 μL) and, after drying, exposed to plasma fed by different gaseous mixtures. The amount of enzyme exposed to the DBD (hereafter the "enzyme loading") was easily varied by changing the enzyme concentration of the drop-casted solution. After the plasma process, the enzymes were re-dissolved in buffer and the reaction rate (rate of production of the colored product) upon addition of a fixed amount of substrate (the reactant in the enzymology jargon) was measured spectrophotometrically. The *residual activity* was determined as the ratio between the reaction rate measured for the enzyme exposed to the plasma and the reaction rate measured for the same quantity of enzyme dried out on the glass slide but not exposed to plasma. The effect of plasma exposure on enzyme kinetics was also investigated for selected plasma processes. In addition to the characterization of enzyme functionality, thickness measurements and XPS analyses of the dry enzyme deposits were carried out before and after plasma exposure.

GOx: residual activity and enzyme deposit thickness

Fig. 1A reports the residual activity of GOx, expressed as a percentage, after exposure for different times to DBDs fed with He and with the He/1% O_2 mixture. Considering the He/O_2-fed DBD, the activity of 30 μg

of GOx drastically decreases to 38% after 10 min exposure, it drops to 15% after 30 min and levels off to such a value for longer exposure times.

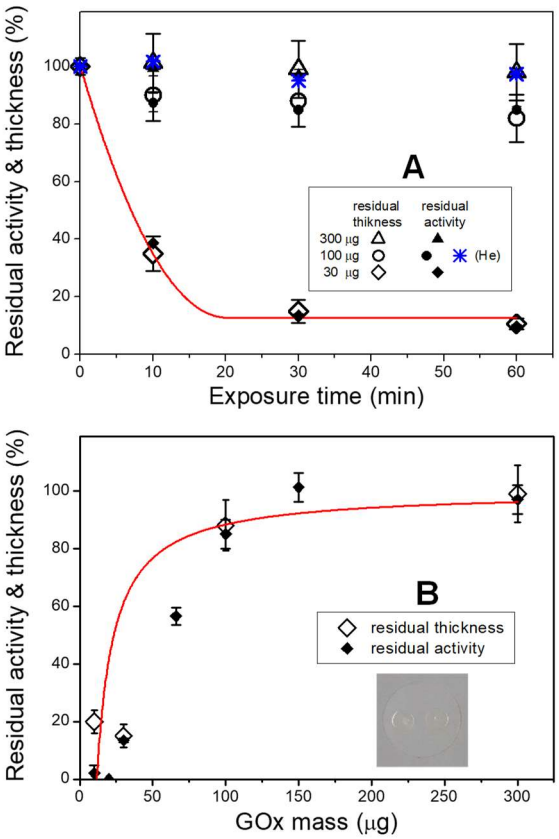

Fig.1 (A) Residual activity (closed symbols) and residual thickness (open symbols) of GOx exposed to DBDs fed with He/1% O_2 mixture or pure He (blue asterisks) for different times; symbols denotes different amounts of GOx (f = 20 kHz, V_a = 1.1 kV_{rms}). The solid line is the best fit to eq. 4 of the residual thickness (30 µg GOx). (B) Residual activity (closed symbols) and residual thickness (open symbols) of different amounts of GOx exposed to the He/1% O_2 fed DBD for 30 min. The solid line is the best-fit to eq. 2. In the inset a representative picture of two dry GOx deposits (100 µg each) onto a glass slide.

The effect is however dependent on the amount of dry enzyme exposed to the DBD. In the case of 100 µg, the activity after 10 min plasma in He/O_2 mixture is still 87%, and upon increasing the exposure time to 60 min it levels off at 85%. At variance with previous results, considering the same GOx amounts the exposure to the pure He plasma for 60 min does not affect the enzyme activity (blue asterisks in **Fig. 1A**). By trebling the amount of exposed enzyme (300 µg), inactivation is negligible and the activity is fully preserved (100%) after 60 min exposure to the He/O_2 DBD. To investigate in more detail the role played by the mass of dry enzyme on the preservation of the enzymatic activity, we kept fixed the exposure time to the He/O_2 DBD at 30 min and varied the enzyme amount between 10 µg and 300 µg. The results are shown in **Fig. 1B** as closed dots. The enzyme activity is preserved for a deposited mass larger than 150 µg while, for lower mass values, a fraction of the enzyme is inactivated and the lower the enzyme initial loading, the lower the residual activity. The drying of the droplet of GOx solution deposited by drop casting on glass slides leads to a roughly circular uniform GOx layer with a diameter of 3.3 ± 0.4 mm, as shown in the picture in **Fig. 1B**. Since the volume of enzyme solution deposited on the glass slides is fixed and the area covered by the protein is constant, the initial thickness (h°) of the enzyme layer will be roughly proportional to the mass of enzyme deposited according to

$$h° \sim \frac{mass}{\rho \times area} \qquad (1)$$

where ρ is the protein density (weight/volume).

The topography of the protein deposits was investigated by means of white light vertical scanning interferometry (WLVSI) before and after plasma exposure. A representative bidimensional (2D) WLVSI image of the pristine 100 µg GOx deposit is shown in **Fig. 2A** and the corresponding cross-section thickness profile (height vs. position) is reported in **Fig. 2C**. The maximum height of the pristine deposit is around 11 µm with a uniform roof. The edge is relatively steep (it develops in less than 20 µm) so that the overall shape can be approximated to a low and wide cylinder whose height is well approximated by eq. 1. The exposure to the He/1% O_2 plasma for 30 min induces a sizeable reduction of the height of the deposit that becomes wrinkled (in particular along the edge) as shown in **Fig.s 2B** and **2C**. This is consistent with a significant removal of the protein through a mechanism of plasma etching. The mean height of the deposit was estimated by averaging the values measured by WLVSI at four different positions along the deposit edge. The residual thickness was determined as ratio between the mean thickness after (h) and before ($h°$) exposure to the plasma.

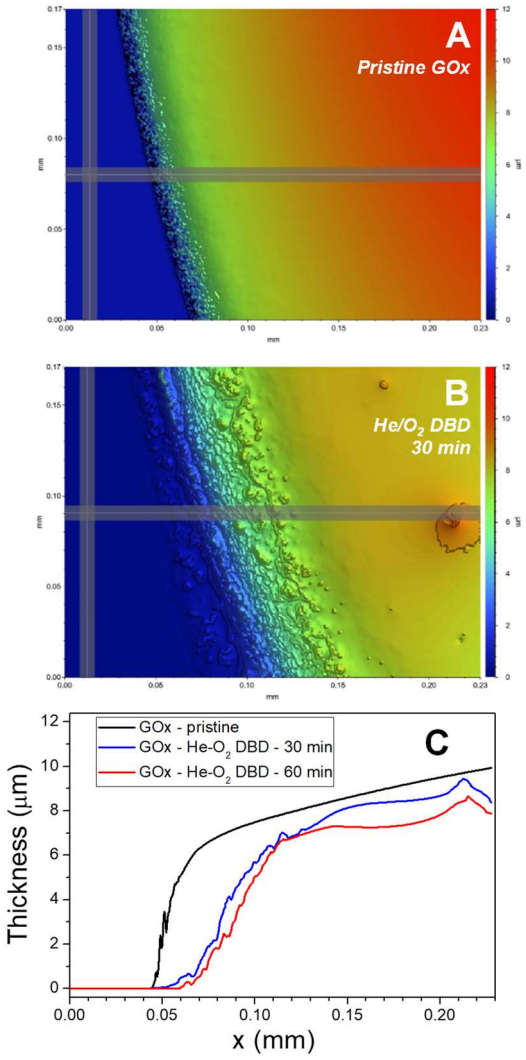

FIG.2 Representative 2D white light vertical scanning inteferometry images of a GOx deposit (100 µg) before (A) and after (B) exposure to a He/1% O_2 fed plasma for 30 min (f = 20 kHz, V_a = 1.1 kV_{rms}). (C)

Cross-section thickness profiles of the GOx deposit before and after exposure to the He/O_2 fed DBD for 30 and 60 min.

The residual thickness values (reported as percentages) are shown as open symbols in both **Fig. 1B**, for experiments at fixed exposure time (30 min) and different deposited GOx amounts, and **Fig. 1A** for experiments at variable exposure time. The result is striking: the residual thickness coincides, within the experimental uncertainty, with the residual activity. This indicates that, in the case of the He/1% O_2 fed plasma, the main reason of the enzymatic activity decrease is the ablation of a fraction of the protein by dry etching. Since the amount of ablated protein should not depend on the height of the protein layer, the thickness of the ablated layer in 30 min (**Fig. 1B**) should be constant with the exposed enzyme amount. Under such an assumption the residual thickness is

$$residual\ thickness = 1 - \frac{d_{30}}{h^\circ} = 1 - d_{30} \cdot \rho \cdot area \frac{1}{mass} \qquad (2)$$

where d_{30} is the thickness of the layer that is ablated in 30 min and the last equality is obtained from eq. 1.

The data of **Fig. 1B** can be fitted to eq. 2 obtaining as best-fit parameter the product $d_{30} \cdot \rho \cdot area$ =1200 ± 200 μg (see the red curve in **Fig. 1B**). Assuming the protein density ρ~1.3 g/mL[27], this corresponds to d_{30}= 1.1±0.3 μm and therefore to an apparent etching rate d_{30}/30 min= 36±14 nm/min. However, the observed dependence of the residual thickness on the plasma exposure time is not compatible with a constant etching rate with time. One hour of ablation at an etching rate of 36 nm/min should remove 2.2 μm. Since the initial height of the layer formed by 100 μg of GOx is 9 μm the residual thickness (and enzymatic activity) should be 75% after one hour and not 82%. Also in the case of the thicker layers formed by 300 μg (15 μm) of GOx, the residual thickness after 60 min should be much less than that experimentally observed value (85 % instead of 98%). The data shown in **Fig. 1A** indicate that the etching rate decreases with exposure time and eventually vanishes after a given time. X-ray photoelectron spectroscopy analyses indicate that the chemical composition of the uppermost layer of protein deposit changes after plasma exposure (*vide infra*) and, therefore, it is conceivable that newly formed chemical species on the enzyme deposit surface generate an etching resistant protective layer, leading to a time-dependent etching rate, v_{et}(t). The data of **Fig. 1A** indicate that after a given time (between 10 and 30 min) the etching process stops. The simplest way to model such behaviour is to assume that the etching rate decreases linearly with the exposure time until vanishes for a time τ according to:

$$\begin{aligned} v_{et}(t) &= -\frac{dh}{dt} = a(\tau - t) && ;t \le \tau \\ v_{et}(t) &= -\frac{dh}{dt} = 0 && ;t > \tau \end{aligned} \qquad (3)$$

where the initial etching rate is $a\tau$. The thickness of the ablated layer (d) is found by integration of the eq. 3, obtaining $d = a\tau t - \frac{a}{2}t^2$ for t ≤ τ and $d = \frac{a}{2}\tau^2$ for t > τ. Considering that the residual thickness depends on the ratio between d and the initial height h° of the protein layer, the following equation describing the dependence of residual thickness on the exposure time to the plasma is obtained

$$\begin{aligned} residual\ thickness &= 1 - \frac{a\tau}{h^\circ}t + \frac{a}{2h^\circ}t^2 && ;t \le \tau \\ residual\ thickness &= 1 - \frac{a}{2h^\circ}\tau^2 && ;t > \tau \end{aligned} \qquad (4)$$

The residual thickness observed at different times for 30 μg of GOx was fitted to eq. 4 (see the red line in **Fig. 1A**) obtaining as best fit parameters a= 0.015±0.001 μm min^{-2} and τ= 20±1 min. It is simple to compare these values with the apparent thickness of the layer that is ablated in 30 min discharge (previously obtained by fitting the data of **Fig. 1B** to eq. 2). Since τ < 30 min, the thickness of the layer ablated during the etching is $d_{30} = \frac{a}{2}t^2$= 3.0±0.5 μm that compares well with the calculations at variable enzyme loading.

GOx enzyme kinetics

In the previous section the enzyme activity was quantified in terms of the rate of product formation at a given concentration of the substrate. This is also the approach used to date in most investigations on

plasma/enzyme interaction.[11,14,28,29] However, modification of the enzyme can affect its activity according to different mode of actions. To grasp this point we considered the simplest case of an enzyme whose initial rate V° obeys the Michaelis-Menten (M-M) equation:

$$V° = \frac{k_{cat}[E][S]}{K_m+[S]} = \frac{V_{max}[S]}{K_m+[S]} \quad (5)$$

Where [S] denotes the substrate initial concentration and k_{cat} the turnover number. For large [S] values, V°~ V_{max}∝ [E] and any inactivation process that reduces the concentration of functional enzymes, [E], decreases the experimental reaction rate. However, an enzyme modification can also impact its affinity for the substrate resulting in different values of the M-M constant (K_m). To explore such a possibility, the initial rates were measured at different substrate concentrations for solutions made dissolving in buffer GOx that was i) only dried, (ii) exposed to He plasma, iii) exposed to plasma fed with the He/1% O_2 mixture. The longest plasma exposure time (60 min) was chosen to emphasize the effects. The GOx loading was fixed to 100 μg as compromise because for lower amounts the residual activity was too low to obtain safe measurements at low [S]-values, while at higher GOx loading the enzyme is essentially unaffected by the plasma process.

Representative M-M plots (V° vs. [S]) are shown in **Fig. 3A** where, in the case of GOx treated in He/1% O_2 plasma, a decrease in the plateau at high [S] (i.e. where V°=V_{max}) is discernible. In all examined cases the V° vs. [S] plots are well accounted for by the M-M eq. 5. The best-fit values are listed in the caption of **Fig. 3A** and in the following we discuss about relative changes, since we are handling an apparent K_m because it is estimated by a bi-enzymatic assay and its numerical value depends on the ratio between GOx and HRP.
The exposure to the He/1% O_2 fed plasma decreases the V_{max} by 16%, in agreement with the observed reduction in activity. With respect to the affinity, while the He plasma does not affect the apparent K_m value, a 36% increase in K_m value is detected after exposure to the He/1% O_2 fed plasma. It is not trivial to assess the significance of such a change because the M-M eq. 5 depends nonlinearly on V_{max} and K_m. To clarify this point we evaluated the correlation between the best-fit parameters through a Monte-Carlo analysis whose results are summarized in **Fig. 3**. In particular, **Fig. 3B** indicates that the uncertainty on V_{max} does not obscure the small decrease in V_{max} (enzyme deactivation) upon exposure to a He plasma and the larger effect of the He/1% O_2 fed plasma. The K_m after the treatment with He DBD is indistinguishable from the control, while the exposure to the He/1% O_2 plasma increases the K_m (see **Fig. 3C**). It is unlikely that such a result is due to the uncertainty in K_m because the inset of **Fig. 3A** shows that V_{max} and K_m are positively correlated. On the contrary, the data of **Fig. 3** demonstrate that the exposure to the He/1% O_2 plasma reduces the V_{max} (inactivates the enzyme) and increases the K_m (reduces the affinity for the glucose of the still functional enzyme).

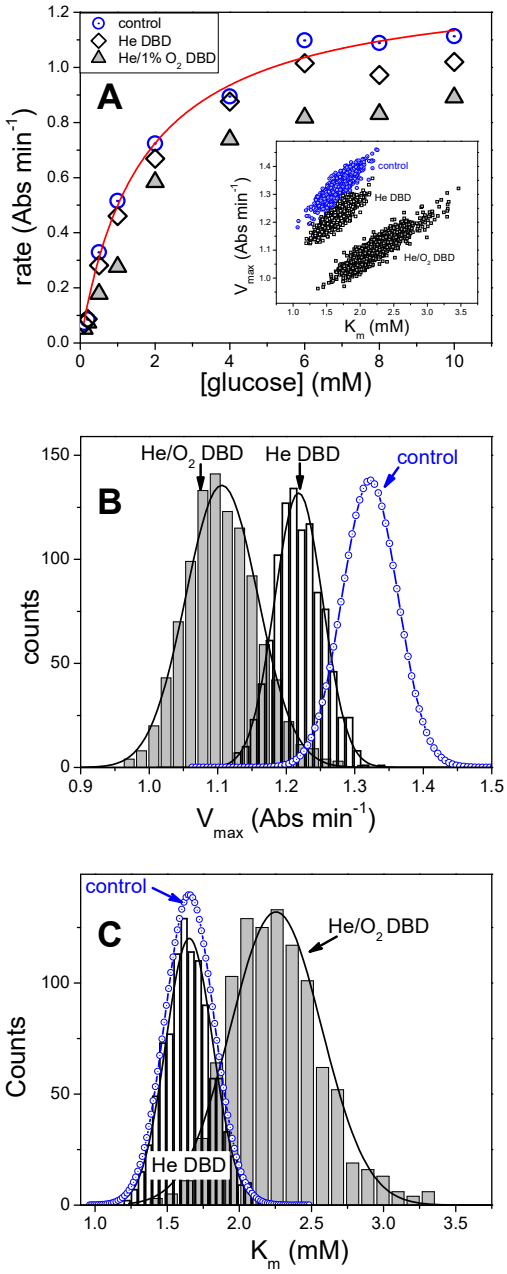

Fig. 3 (A) Initial rates as a function of the initial glucose concentration obtained for 100 µg of GOx redissolved in buffer after: drying (the control dotted circle), exposure to He plasma for 60 min (open diamond), exposure to He/1% O_2 plasma for 60 min (grey triangle). DBD excitation conditions: f = 20 kHz, V_a = 1.1 kV_{rms}. The data were fitted to eq. 5 (for the sake of clarity only the fit to the control is shown) giving the following best-fit parameters: control K_m = 1.6±0.2 mM, V_{max} = 1.32±0.04 Abs/min; exposed to He plasma K_m = 1.6±0.2 mM, V_{max} = 1.22±0.03 Abs/min; exposed to He/O_2 plasma K_m = 2.2±0.3 mM, V_{max} = 1.10±0.05 Abs/min. The results from 1000 runs of Monte Carlo analysis of data in panel A are shown in the inset of panel A (correlation between the V_{max} and K_m best-fit values), in panel B (frequency of the V_{max}) and in panel C (frequency of the Michaelis constant K_m).

Surface chemical characterization of GOx deposits

As a whole, the above discussed data point to a plasma-induced drastic modification of the surface of the protein deposit. In the case of the plasma fed with the He/1% O_2 mixture such a modification consists in the

etching and oxidation of the aminoacids and eventually seems to lead to an inert "crust" that halts the etching itself.

The XPS results reported in **Table 1** show that after 30 min treatment with the pure He DBD both nitrogen and oxygen surface atomic concentrations decrease and, consequently, the carbon concentration increases (+9%) along with the atomic percentages of impurities (mainly K and Na,+1.7%). Accordingly, the curve fitting of the high-resolution C 1s signal (**Table 1**, **Figure S1**) indicates a drop of the peak area percentages of the components due to C-N/C-O (-12%) and C=O/O-C-O (-11%) groups, and a concomitant increase (+22%) of the hydrocarbon component at 285.0 eV. Interestingly, the O 1s and N 1s signals do not significantly change after exposure to the He fed DBD (**Table S2**, **Figure S2**). Specifically, the curve fitting of the O 1s signal does not show changes in the relative amounts of the components due to single (63%) and double-bounded (37%) oxygen, while the N 1s signal remains dominated by the component due to N-C groups present, for instance, in the protein polypeptide backbone. These results indicate that the interaction with the He fed plasma promotes the removal of the nitrogen and oxygen-containing functionalities at the surface of the protein deposit.

Differently, the interaction of the protein with the He/1% O_2 fed plasma for 30 min mainly leads to the increase of atomic oxygen surface concentration (+8%), and consequently to the reduction of carbon (-12%) and nitrogen (-2.2%) atomic percentages. An increase of the surface atomic concentrations of impurities is also observed. According to the curve fitting of the C 1s and O 1s signals (**Tables 1** and **S1**, **Figures S1** and **S2**), the He/1% O_2 fed plasma increases the fraction of C=O/O-C-O and COO groups (as a whole +6%), with a consequent reduction of the C-C/C-H bonds (-8%). The high resolution N 1s signal is dominated by the N-C component (ca. 80%) also after exposure to an oxygen-containing DBD; however, a slight increase of the contribution of C=N bonds is observed as well as the appearance of a new weak component at 407 eV ascribed to oxidized nitrogen (**Table S2**, **FiguresS2**). Considering the reduction of the etching rate with exposure time to a He/1% O_2 fed DBD we observed in our work, it is reasonable to assume that the chemical nature of this surface layer is less prone to etching and thus acts as a protective "crust" that leaves intact the underneath proteins during prolonged plasma processes.

Table 1. XPS surface atomic concentrations and curve fitting results of high-resolution C 1s XPS spectra of the dry GOx and Tyr deposits before and after 30 min exposure to DBDs fed with pure He and the He/1% O_2 mixture (20 kHz, 1.1 kV_{rms}).

	C at%	O at%	N at%	K, Na at%	S, P, F at%	C 1s 1 C-C/C-H peak area%	C 1s 2 C-N/C-O peak area%	C 1s 2 C=O/O-C-O peak area%	C 1s 4 COO peak area%
Glucose oxidase (GOx)									
Pristine GOx	62	27	8.2	2.8	-	40	43	17	-
GOx - He DBD	71	21	3.5	4.0	0.5	62	31	7	-
GOx - He/1% O2 DBD	50	35	6.0	8.5	0.5	32	45	19	4
Tyrosinase (Tyr)									
Pristine Tyr	64	26	8.5	1.0	0.5	37	46	17	-
Tyr - He DBD	47	27	6.5	11.0	8.5	59	27	14	-
Tyr - He/1% O2 DBD	44	37	7.5	7.5	4.0	32	41	20	7

Tyrosinase: residual activity and enzyme deposit thickness

An analogous study was performed on the enzyme tyrosinase revealing a very different scenario. The impact of plasma on the Tyr activity was very weak and became quantifiable only at extremely low enzyme loading. Representative data are reported in **Fig. 4A** where the residual activity of Tyr is shown as a function of the exposure time to DBDs fed with pure He and with the He/1% O_2 mixture. The action of the He/1% O_2 plasma for 10 min on an amount of Tyr of only 5 μg reduces to 85% its activity. After 30 min of plasma

exposure the residual activity is further reduced to 67 % and levels off to such a value for longer exposure times. Decreasing the amount of enzyme to 2 µg does not change such a result, while the use of a pure He plasma reduces the inactivation (82% active) independently from the exposure time. Therefore, Tyr responds to the plasma in a very peculiar way: at very low amounts it preserves its activity also when exposed to the plasma for long time and shows also a very weak dependence of its residual activity on the amount of exposed enzyme.

In this respect, it should be noticed that GOx and Tyr behave differently upon drying. Indeed, GOx gives raise to a uniform dry deposit (**Fig. 1B**) while Tyr develops an evident coffee ring as shown in the picture in **Fig. 4A**.

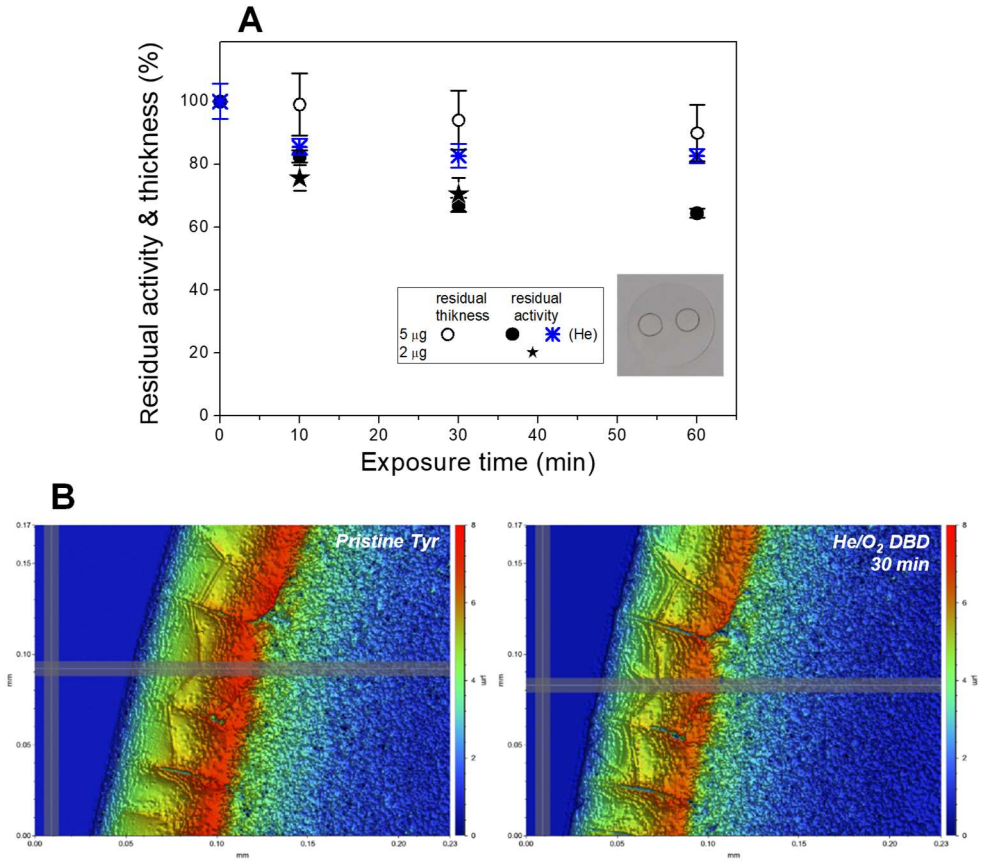

Fig. 4 (A) Residual activity (closed symbols) and residual thickness (open symbols) of tyrosinase exposed to DBDs fed with He/1% O_2 mixture or pure He (blue asterisks) for different times (f = 20 kHz, V_a = 1.1 kV_{rms}). The residual activity is plotted for both 2 and 5 µg of enzyme. In the inset a representative picture of two 5 µg Tyr deposits onto a glass slide. (B) 2D WLVSI images of a 5 µg Tyr deposit before and after exposure to a He/1% O_2 fed DBD for 30 min (f = 20 kHz, V_a = 1.1 kV_{rms}).

The non-homogeneous distribution of the dry Tyr leads to an annular deposit whose morphology was investigated by means of WLVSI before and after the plasma process. A representative 2D WLVSI image of the pristine deposit of 5 µg is shown in **Fig. 4B** where the presence of inhomogeneities and fractures perpendicular to the perimeter of the coffee ring are visible. **Fig. 4B** reports also the WLVSI image of the sample at the same position after exposure to He/1% O_2 plasma for 30 min. The mean height of the deposit was estimated by averaging the values measured at four different regions of the sample on top of the coffee ring and the residual thickness has been evaluated for samples exposed for different time to He/1% O_2

plasma. The residual thickness data, shown as open symbols in **Fig.4A**, reveal an extremely weak decrease upon exposure to the He/1% O_2 plasma. After 60 min of treatment the residual thickness is still 90% while the residual enzymatic activity is reduced to 64%. Therefore, in the case of 5 μg of dry tyrosinase we obtained sizeable attenuation of the enzyme activity but only a minor decrease in the thickness of the enzyme deposit (see for comparison thickness profiles obtained from WLVSI images in **Figure S4**).

Tyr enzyme kinetics

The M-M curves and the V_{max} and K_m values for the control and for the enzyme exposed to He/1% O_2 plasma were determined also for the tyrosinase. Enzyme exposure to pure helium plasma was not considered since it scarcely affects the tyrosinase activity.

Representative M-M plots are shown in **Fig. 5A** where an evident decrease in the plateau at high [S] is discernible for the Tyr treated in He/1% O_2 plasma. In all the cases the V° vs. [S] plots are well accounted for by the M-M eq. 5. The best-fit values are V_{max}= 0.39±0.01 Abs min^{-1} and K_m= 0.32±0.04 mM for the control and V_{max}= 0.30±0.01 Abs min^{-1} and K_m= 0.29±0.04 mM for the enzyme exposed to the plasma. A Monte-Carlo analysis of the fit of the M-M eq. 5 to the data indicates that the 23% decrease V_{max} is statistically relevant (**Fig. 5B**), the small decrease in K_m after the exposure to the He/1% O_2 plasma (**Fig. 5C**) is likely due to the statistical positive correlation between V_{max} and K_m shown in the inset of **Fig. 5A**.

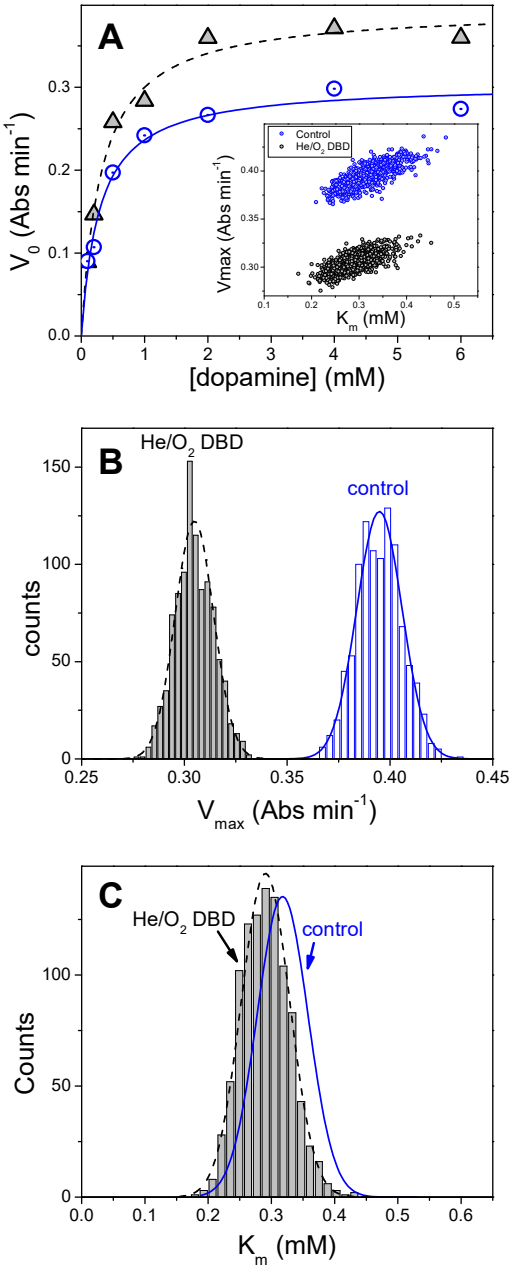

Fig. 5. A) Initial rates as a function of the initial dopamine of 5 μg of tyrosinase redissolved in buffer after: desiccation (the control dotted circle), exposure to He/1% O_2 plasma for 30 min (grey triangle). DBD excitation conditions: f = 20 kHz, V_a = 1.1 kV_{rms}. Lines are the fit to eq. 5; best-fit parameters: control K_m = 0.32±0.04 mM, V_{max} = 0.39±0.01 Abs/min; exposed to He/O_2 plasma K_m = 0.29±0.04 mM, V_{max} = 0.30±0.01 Abs/min. The results from 1000 runs of Monte Carlo analysis of data in panel A are shown in the inset of panel A (correlation between the V_{max} and K_m best-fit values), in panel B (frequency of the V_{max}) and in Panel C (frequency of the Michaelis constant K_m).

Surface chemical characterization of Tyr deposits

Table 1 shows that, in the case of Tyr, the 30 min treatment with He plasma induces a reduction of the carbon atomic concentration (-17%) and a slight decrease of the nitrogen percentage, while a consistent increase of the impurities concentrations occurs. The discussion of XPS data is somehow complicated by the appearance of these contaminations that distort the atomic percentages of C, O and N. Nevertheless, focusing

the attention on the high resolution spectra, it is possible to identify more precisely changes induced by plasma exposure.
First of all, the curve fitting of the C 1s signals reveals that the exposure to a He DBD leads to a reduction of the components due to C-O/C-N (-19%) and to C=O/O-C-O (-3%) groups, with a a concomitant increase (+12%) of the hydrocarbon component at 285.0 eV (**Tables 1 and S2, Figure S5**). The curve fitting of the O 1s signals shows that the relative amount of double-bonded oxygen increases (+18%) at the expense of single-bounded oxygen; while slight changes are observed in case of the N 1s signal dominated by the C-N component at about 400.0 eV (80%). Therefore, in case of tyrosinase, the interaction with the He fed plasma primarily induces the loss of nitrogen and carbon as well as bond rearrangements mainly involving the residual carbon and oxygen atoms. Differently, a loss of both nitrogen- and oxygen-containing functionalities was observed for GOx, together with an increase of the carbon content and, more precisely, of the hydrocarbon component (C 1s curve fitting, **Table 1**, **Figure S1**).
As also observed for GOx, the interaction of the He/1% O_2 plasma with the dry Tyr deposit mainly results in the implantation of oxygen, with a 11% increase of its XPS surface concentration and a consequent reduction of carbon atomic percentage (**Table 1**). The similarity of the surface chemical composition of Tyr and GOx deposits after exposure to the oxygen-containing DBD is also confirmed by the curve fitting of the high-resolution C 1s signals (**Table 1**, **Figure S5**). In the case of Tyr, in fact, a reduction in the hydrocarbon and C-N/C-O components (as a whole, -10%) is observed accompanied by an increase of the peak area percentages of components ascribed to C=O/O-C-O and carboxyl functional groups. Interestingly, minor changes in the Tyr N 1s signal are detected after exposure to the He/1% O_2 fed DBD (**Table S3**).

Overcoating by a polyethylene-like film

In the case of DBDs fed with helium-ethylene mixture, an uniform polyethylene-like coating is deposited on the dry enzyme (see FTIR and XPS characterization in the supporting information). Such a hydrophobic coating (static water contact angle of about 100°) acts as an efficient barrier precluding the release of the enzyme when immersed in the solution. As an example, in **Fig. 6A** the time course of the GOx activity assay is shows in the case of the untreated enzyme (in black) and of the GOx deposit overcoated by a 270 nm polyethylene-like film (in red), assayed according to the experimental section. The introduction in solution of 50 μg of untreated dry GOx immediately triggers the sequence of reactions that lead to an increase in the absorbance at 420 nm while, in the case of the same amount of GOx overcoated by the plasma polymer, the reactions do not take place. After 9 min of immersion, the polyethylene-like film is gently scratched allowing the release of the underneath enzyme eliciting instantly the GOx-catalysed glucose oxidation.
Since the slope of the trace after the scratching is the same of the initial slope for the untreated enzyme, in this case the residual activity is around 100%. Indeed, the PE-CVD from ethylene-containing DBD has only a minor impact on the activity of the underneath enzyme. In the Inset of **Fig. 6A** the GOx residual activity observed after 30 min of PE-CVD at different ethylene content in the feed mixture is reported. The activity is only slightly reduced (~90%) in comparison with the untreated sample when an applied voltage of 1.1. kV_{rms} is used for DBD generation, but can it be fully retrieved by decreasing the applied voltage to 0.85 kV_{rms}.
The exposure time turned out to be a critical parameter for preserving the enzyme functionality in the case of Tyrosinase (5 μg), as shown in **Fig. 6B**. The exposure to the helium/ethylene DBD for 30 min reduces the residual activity to ~80% independently from the applied voltage (1.1 kV_{rms} or 0.85 kV_{rms}) and the ethylene concentration in the feed mixture (from 0.3% to 1.0%). However, the reduction of the PE-CVD process duration to 10 min fully retrieves the enzyme activity.

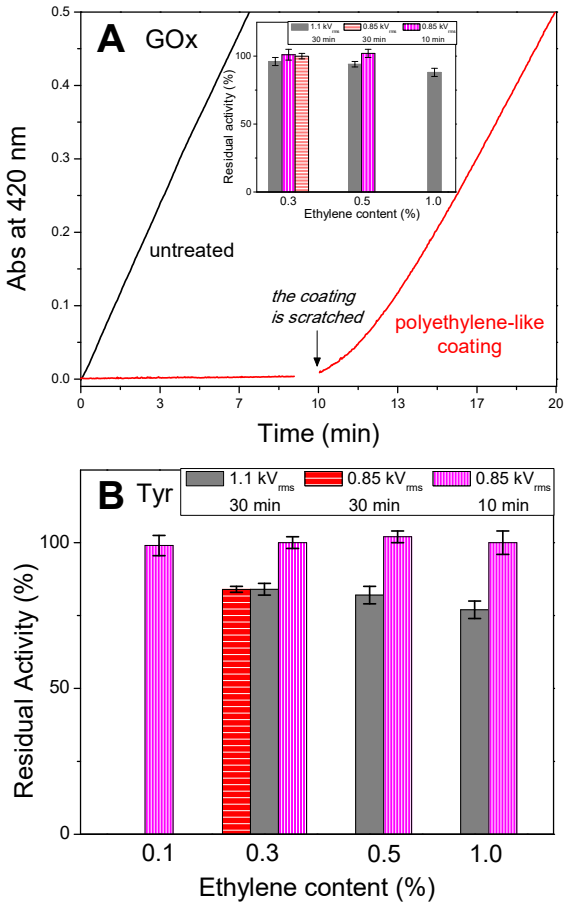

Fig. 6 (A) Time evolution of the absorbance at 420 nm following the immersion of glass slide with an untreated dry GOx deposit (black line) and with a GOx deposit coated by the polyethylene-like thin film (red line). In the latter case, after 9 min the coating was scratched. Inset: residual activity of GOx (50µg) after coating with the polyethylene-like thin film deposited by DBD under different conditions (f = 20 kHz, V_a= 850, 1100 V_{rms}, [ethylene] = 0.3, 0.5 and 1%). (B) Residual activity of Tyr (5 µg) after coating with a polyethylene-like thin film deposited under different conditions (f = 20 kHz, V_a= 850, 1100 V_{rms}, [ethylene] = 0.1, 0.3, 0.5 and 1%).

Plasma impact on dry enzymes: comparison between GOx and Tyr

The response of the two enzymes to plasma exposure reveals some quantitative differences. The GOx loss of functionality upon exposure to the He/1% O_2 DBD is directly correlated to the deposit thickness decrease due to the dry etching. The chemical modification of the enzyme deposit surface reasonably results in the formation of a "crust" with strong ablation resistance which, under the experimental conditions utilized in this work, progressively reduces the etching rate. To minimize the loss of enzyme functionality it is necessary to expose to the plasma a thick protein layer and, therefore, large amounts of GOx are required (hundreds of µg).

The behavior of tyrosinase is different. Deposits corresponding to more than 10 µg of dry protein are insensitive to He/1% O_2 plasma, while layers prepared depositing very low amounts of Tyr (5-2 µg) show a small but sizeable attenuation of the enzyme activity and only a minor decrease in the deposit thickness.

There are two possible explanations for this different enzyme response upon exposure to the oxygen-containing DBDs:

i) The first explanation is that GOx is more prone to be ablated by the oxygen-containing plasma compared with Tyr that reveals an effect of the exposure to the plasma only at very low protein concentration. At this low enzyme loading (at which the oxygen-containing plasma totally inactivates the GOx) the attenuation of Tyr activity is larger than the thickness loss of the Tyr deposit suggesting that the enzyme somehow resists to etching reactions but it seems more prone to be inactivated by the plasma reactive species. However, the analysis of the impact of the oxygen-containing plasma on the enzyme affinity (K_m) for the substrate points in the opposite direction. Indeed, we observe a sizeable reduction of the affinity in the case of the GOx but not for Tyr.
A drastically different reactivity with the plasma for the two proteins seems unlikely because the final surface chemical composition in terms of bonds involving carbon, oxygen and nitrogen seems to be very similar for the two enzymes after exposure to the He/O_2 plasma (**Tables 1**, **S2** and **S3**). This suggests that the reactions involving the protein framework and plasma-generated reactive species are the same and for both enzymes the etching process stops when a given surface structure has been formed.

ii) A different explanation is based on the morphology of the solid deposit that the two proteins form. In the case of the uniform layers formed by GOx, the amount of ablated protein is mirrored by the decrease in the enzyme activity. It can be noted that the ablation is larger on the discontinuities along the deposit rim (Fig. 2) but since this involves a small fraction of the deposit the overall effect is only a decrease in the thickness of the protein layer. In contrast, in the case of the coffee ring formed by the dry Tyr, the rim represents a large fraction of the deposit. In addition, the cracks and fractures crossing the annular Tyr deposit seem to act as preferential path for the oxygen-containing plasma (**Fig.s 4B and S4**) and increase their width and depth upon plasma exposure. The overall result is that a quantifiable part of enzyme is ablated from the edge and within the cracks leaving almost unchanged the height of the top of the deposit.

CONCLUSIONS

The reactive environment generated in an atmospheric pressure cold plasma strongly interacts with the outermost layers of dry enzyme deposits. However, such an interaction runs out at most within the first few micrometers of the enzyme deposit. It is thus feasible to make negligible the activity reduction by increasing enough the thickness of the initial enzyme deposit either by increasing the enzyme loading or by tailoring a non-uniform enzyme deposition (e.g., a coffee ring shape). There is a wide literature that point out to a strong plasma-induced inactivation of the enzymes in an aqueous environment associated to the formation of water soluble reactive species such as H_2O_2, hydroxyl radicals and so on.[18,19,30,] The results of the present study suggest that the high stability of dry enzymes exposed to plasma is because these routes of inactivation found in solution are absent in the solid state and, therefore, allow envisaging new and unexpected directions towards surface engineering of enzymes through plasma-based approaches.
We emphasize that sizeable destruction of the enzyme was achieved only in the case of an oxygen-containing feed mixture, for relatively harsh conditions of applied voltage (1.1 kV_{rms}) and very long exposure time (> 30 min). Instead, the customary conditions used for PE-CVD with atmospheric pressure cold plasmas fed with helium/ethylene mixtures (applied voltage < 1.1 kV_{rms} and exposure time ≤ 10 min) can be considered friendly for the dry enzymes and this open the way to time saving strategies of immobilization of known amount of enzymes (in well-known ratios) by easy overcoating.

EXPERIMENTAL SECTION

Reagents

Glucose Oxidase from Aspergillus Niger (Type II, ≥15,000 enzyme units/g solid), Tyrosinase from Mushroom (≥1000 unit/mg solid), Peroxidase from Horseradish (Type VI-A, 950-2000 enzyme units/mg solid), Tris Hydrochloride and Dopamine hydrochloride were purchased from Sigma-Aldrich. D-(+)-Glucose, di-Sodium hydrogen phosphate and Sodium di-hydrogen phosphate were bought from Fluka, while ABTS was from VWR Amresco. Compressed helium (99.9995%) and oxygen (99.999%) gas cylinders were purchased from Sol, while ethylene (99.95%) was purchased from Airliquide.

DBD reactor setup and plasma processes

Plasma processes were carried out using a home-built atmospheric pressure dielectric barrier discharge (DBD) reactor, as described elsewhere in full detail.[31,32] The plasma was generated between two parallel plate electrodes (4 mm gas gap, 50×50 mm^2 electrode area) both covered with a 0.635 mm thick Al_2O_3 plate (CoorsTek, 96%), by applying a sinusoidal ac high voltage. Experiments were carried out at the fixed excitation frequency (f) of 20 kHz and applied voltages (V_a) of 0.85 and 1.1 kV_{rms}. The voltage applied to the electrodes was measured by means of a high-voltage (HV) probe (Tektronix P6015A), while the current flowing through the electrical circuit was evaluated by measuring the voltage drop across a 50 Ω resistor in series with the ground electrode (Tektronix P2200 voltage probe). The average specific power dissipated by the discharge (P_s) was calculated as the integral over one cycle of the product of the applied voltage and the current, divided by the period and the electrode area.

The DBD electrode system was located into an airtight Plexiglas chamber (volume of about 14 L) slightly pumped by a dry diaphragm pump (Pfeiffer) to keep the working pressure constant (10^5 Pa), as measured by a MKS capacitive pressure gauge. Plasma processes were carried out using DBDs fed with He, He-O_2 and He-C_2H_4 mixtures. The feed gas was introduced in the discharge zone through a slit and pumped through a second slit positioned on the opposite side (i.e., lateral gas injection). The gas flow rates were regulated and measured by MKS mass flow controllers (MFC). He flow rate was kept fixed at 8 slm, O_2 concentration in He-O_2 mixture was equal to 1% (hereafter referred to as He/1% O_2 mixture) while ethylene concentration in He-C_2H_4 mixtures was varied in the range 0.1 – 1%. Before each experiment, the Plexiglas chamber was purged with 6 slm of He for 20 min to remove air contaminations. During the plasma processes, the samples were placed in the middle of the discharge region, onto the Al_2O_3 plate covering the lower electrode. The process duration (t) was varied between 10 min and 60 min. The experimental conditions utilized in the present study are detailed in the Supporting Information.

Sample preparation, treatment and enzyme functionality assay

5 μL drops of the selected enzyme, in the suitable buffer and concentration, were deposited on a coverglass slide (12 mm diameter and 0.15 mm thickness) and dried under reduced pressure for 30 min.

A set of slides was prepared and retained to be used as control while a second set was placed in the DBD reactor and exposed to the selected plasma process. After that, each slide was separately immersed in a 1 mL of buffer. Solubilisation of enzymes occurred under slight stirring in few seconds, then enzymes could be assayed for their activity. In the case of discharge from helium-ethylene a very hydrophobic polyethylene-like coating, covering and keeping underneath the enzyme, was deposited. The coating was then scratched using a polypropylene pipette tip, allowing the release of the entrapped enzyme and its solubilisation.

After solubilisation, the enzyme activity was evaluated by means of spectrophotometric assays (by using a Jasco V-530 spectrophotometer). For the activity measurements, a known amount of substrate (at concentration >> K_m) was added to both control and plasma treated enzymes, then the rates of absorbance growth were measured and could be compared. Reaction rates are always expressed as absorbance min^{-1}.

In the case of glucose oxidase, the glucose was the substrate and the activity was probed by exploiting the classical bienzymatic assay involving both the GOx and the horseradish peroxidase (HRP). In this assay, the hydrogen peroxide produced by the GOx-catalysed glucose oxidation is the substrate of the HRP and is used

to oxidize the leuco dye ABTS to a colored product, whose formation can be probed at 420 nm[33]. In the case of tyrosinase, dopamine was used as the substrate and the increase in absorbance at 475 nm, due to dopaminechrome formation, was measured[34].

For selected plasma process conditions, the full Michaelis-Menten plot (initial rate vs substrate concentration) were obtained and the Michaelis-Menten constant (K_m) as well as the maximum velocity (V_{max}) were determined. Since the points of the full Michaelis-Menten plot (including the replicates) must be obtained with exactly the same enzyme concentration, several dry enzyme samples were exposed to the plasma in the same process and, subsequently, pooled to obtain a large volume enzyme solution from which aliquots were withdrawn to be assayed.

The error estimation of the parameters obtained by the fits was performed by means of Monte Carlo simulation with the OriginPro package (OriginLab Corporation) using a suitable worksheet script. The overall approach was as follows. The parameters obtained by fitting the set of experimental data to the Michaelis–Menten function (Eq. (5)) were used to create "perfect" (noise free) data sets. Random noise, corresponding to the standard deviation obtained by the best-fit of the experimental data, was added to the perfect data set. The data were then fitted by a least-squares routine to Eq. (5). This process was repeated 1000 times, taking care to add a different set of noise to the perfect data before each cycle. The best-fit parameters were analyzed for the mean and standard deviation.

Further details on buffers, substrate concentrations etc. are given in the Supporting Information.

X-ray photoelectron spectroscopy (XPS) analyses

XPS analyses were performed using a PHI VersaProbe II spectrometer equipped with a monochromatic Al Kα X-ray source (1486.6 eV) operated at a spot size of 100 μm corresponding to a power of 24.5 W. Survey (0−1400 eV) and high resolution (C 1s, O 1s, N 1s, S 2p, K 2p, Na 1s, P 2p, F 1s) spectra were recorded in FAT (fixed analyzer transmission) mode at pass energy of 117.4 and 46.95 eV, respectively. All spectra were acquired at a take-off angle of 45° with respect to the sample normal. Dual-beam charge neutralization was constantly applied during analysis. Special care was devoted to verify that no change in the samples was induced by exposure to the X-ray beam and to the dual-beam used for charge neutralization. Detailed spectra processing was performed by commercial MultiPak software (Version 9.5.0.8, 30-10-2013, Ulvac-PHI, Inc.). Charge correction of the spectra was performed by taking the hydrocarbon component of the C 1s spectrum as internal reference (binding energy, BE = 285.0 eV). The high-resolution C 1s, O 1s and N 1s spectra were fitted with mixed Gaussian-Lorentzian peaks after Shirley background subtraction. Details on the curve fitting components are reported in the Supporting Information. The uncertainty associated with peak position was estimated to be ±0.2 eV. The full width at half-maximum (FWHM) of each C 1s, O 1s and N 1s line shape was allowed varying in the range 1.3-1.6 eV, 1.5-1.7 eV and 1.5-1.7 eV, respectively. For each enzyme, analyses were repeated on two samples (at least three points per sample) treated by DBD in two different experiments. A maximum relative standard deviation of 10% was estimated on the surface atomic concentrations and on the area percentages of the curve-fitting components.

White light vertical scanning interferometry (WLVSI) and stylus profilometry.

White light vertical scanning interferometry was utilized for three-dimensional imaging of dried enzyme deposits and to determine their thickness before and after plasma processes. Analyses were carried out using a Bruker Contour GT-K0X 3D optical microscope equipped with a 50x Mirau-type inteferometric objective and a 0.55x camera zoom (field of view of 0.23 x 0.17 mm^2). In particular, the thickness of the enzyme deposits was measured at four fixed locations (6 measurements per location) along the deposit edge, before and after the plasma processes.

The thickness of the hydrocarbon polymer films deposited by He/C_2H_4 DBD onto borosilicate glass slides was determined using a stylus profiler (KLA-Tencor Alpha-Step® D-120). After the plasma process, the coating was scratched off the glass slide with a scalpel blade and thickness measurements were carried out at 5 different positions.

ASSOCIATED CONTENT

Supporting Information

Detailed list of the experimental conditions of plasma processes; additional details on sample preparation, treatment and enzyme functionality assay; high resolution XPS spectra of GOx deposits before and after plasma exposure; additional WLVSI results for Tyr deposits; High resolution XPS spectra of Tyr deposits before and after plasma exposure; Chemical characterization of the coating deposited by DBDs fed with He/C_2H_4 mixtures. This material is available free of charge via the Internet at http://pubs.acs.org.

AUTHOR INFORMATION

Corresponding Authors

* Email: gerardo.palazzo@uniba.it

ORCID

Fiorenza Fanelli: https://orcid.org/0000-0001-9738-6648

Francesco Fracassi: https://orcid.org/0000-0003-2037-7772

Antonia Mallardi: https://orcid.org/0000-0001-6926-3958

Gerardo Palazzo: https://orcid.org/0000-0001-5504-2177

Notes

The authors declare no competing financial interest.

ACKNOWLEDGMENT

This paper is dedicated to the memory of our mentor Prof. Riccardo d'Agostino, who recently passed away. Teresa Lasalandra and Savino Cosmai are gratefully acknowledged for the skillful technical assistance. This research was supported by the Italian Ministry for Education, University and Research (MIUR) under grant PONa3_00369 – "Laboratorio SISTEMA", and by Regione Puglia under grant no. 51 - "LIPP" within the Framework Programme Agreement APQ "Ricerca Scientifica", II atto integrativo - Reti di Laboratori Pubblici di Ricerca.

REFERENCES

[1] Grotzky, A.; Altamura, A.; Adamcik, J.; Carrara, P.; Stano, P.; Mavelli, F.; Nauser, T.; Mezzenga, R.; Schlüter, A.D.; Walde *Langmuir* **2013**, *29*, 10831-10840

[2] Mallardi, A.; Angarano, V.; Magliulo, M.; Torsi, L.; Palazzo, G. *Anal. Chem.* **2015**, 87, 11337-11344.

[3] Küchler, A.; Adamcik, J.; Mezzenga, R.; Schlüter, A.D.; Walde, P. *RSC Adv.*, **2015**, *5*, 44530-44544

[4] Sun, L.; Gao, Y.; Xu, Y.; Chao, J.; Liu, H;. Wang, L.; Li, D.; Fan, C. *J. Am. Chem. Soc.* **2017**, *139*, 17525-17532 DOI: 10.1021/jacs.7b09323

[5] Küchler, A.; Yoshimoto, M.; Luginbühl, S.; Mavelli, F.; Walde, P. *Nature Nanotech.* **2016**, 11, 409-420.

[6] Homaei, A.A.; Sariri, R.; Vianello, F.; Stevanato, R. *J. Chem. Biol*. **2013**, *6*, 185-205.

[7] Di Cosimo, R.; Mc Auliffe, J.; Poulose, A; Bohlmann, G. *Chem. Soc. Rev*. **2013**, *42*, 6437–6474.

[8] Heyse, P.; Van Hoeck, A.; Roeffaers, M.B.J.; Raffin, J.-P.; Steinbüchel, A.; Stöveken, T.; Lammertyn, J.; Verboven, P.; Jacobs, P.A. ; Hofkens, J.; Paulussen, S.; Sels, B.F. *Plasma Process. Polym.* **2011**, *8*, 965–974.

[9] Palumbo, F.; Camporeale, G.; Yang, Y.-W.; Wu, J.-S.; Sardella, E.; Dilecce, G.; Calvano, C.D.; Quintieri, L.; Caputo, L.; Baruzzi, F.; Favia P. *Plasma Process. Polym.* **2015**, *12*, 1302–1310.

[10] Liu, Y.-H.; Yang C.-H.; Lin T.-R.; Cheng, Y.-C., *Plasma Process Polym.* **2018**, 1800001 in press.

[11] Marcela M. Bilek, M.M.; McKenzie D. R. Biophys. Rev. **2010**. *2*, 55–65.

[12] Ghasemi, M.; Minier, M. J. G.; Tatoulian,M.; Chehimi, M.M.; Arefi-Khonsari, F. *J. Phys. Chem. B* **2011**, *115*, 10228–10238.
[13] Mertens, N.; Mahmoodzada, M.; Helmke, A.; Grunig, P.; Laspe, P.; Emmert, S; Viöl W. *Plasma Process Polym.* **2014**, *11*, 910–920.
[14] Keidar, M.; Walk, R.; Shashurin, A.; Srinivasan, P; Sandler, A; Dasgupta, S; Ravi, R; Guerrero-Preston, R.; Trink, B. *British J. Cancer* **2011**, *105*, 1295–1301
[15] Keidar, M. *Plasma Sources Sci. Technol.* **2015**, *24*, 033001
[16] Zhang, H.; Xu, Z.; Shen J.; Li, X.; Ding, L.; Ma, J.; Lan, Y.; Xia, W; Cheng, C.; Sun, Q.; Zhang, Z.; Chu P.K. *Sci Rep.* **2015**, *5*, 10031.
[17] Weltmann K.-D., Woedtke, T. *Plasma Phys. Control. Fusion* **2017,** *59*, 014031.
[18] Thirumdas, R.; Sarangapani, C.; Annapure U.S. *Food Biophys.* **2015**, 10, 1-11
[19] Misra, N.N.; Pankaj, S.K.; Segat, A.; Ishikawa, K. *Trends Food Sci. Technol*. **2016**, *55*, 39-47
[20] Baxter, H.C.; Campbell, G.A.; Whittaker, A.G.; Jones, A.C., Aitken, A.; Simpson, A.H., Casey, M.; Bountiff, L.; Gibbard, L.; Baxter, L. *J. Gen. Virol.* **2005**, *86*, 2393-2399
[21] Muguruma, H.; Hoshino, T.; Nowaki, K.; *ACS Appl. Mater. Int.* **2015**, 7, 584−592
[22] Chun Ming Wong & Kwun Hei Wong & Xiao Dong Chen Glucose oxidase: natural occurrence, function, properties and industrial applications Appl Microbiol Biotechnol (2008) 78:927–938
[23] García-Borrón, J.C., Solano, F., 2002. Pigment Cell Res. 15, 162–173.
[24] Simon, J.D., Peles, D., Wakamatsu, K., Ito, S., 2009. Pigment Cell Melanoma Res. 22, 563–579.
[25] Muguruma, H.; Kase, Y. *Biosens. Bioelectr.* **2006**, *22*, 737-743
[26] Fanelli, F.; Fracassi, F. *Surf. Coat. Technol.* **2017**, *322*, 174–201
[27] Fischer, H.; Polikarpov, I.; Craievich, A.F. *Protein Sci.* **2004**, *13*, 2825–2828
[28] Pankaj, S.K.; Misra, N.N.; Cullen P.J. *Inn*. *Food Sci*. *Emerging Technol*. **2013**, *19*, 153–157
[29] Segata, A.; Misra, N.N.; Cullen, P.J.; Innocente, N. *Food Bioprod. Process.* **2013**, *98*, 181–188
[30] Attri, P.; Kim, M.; Sarinont, T.; Choi, E.H.; Seo, H.; Cho, A.E.; Koga, K.; Shiratani, M. *Scientific Reports* **2017**, 7, 8698
[31] Fanelli, F.; Fracassi, F.; d'Agostino, R. *Plasma Process. Polym.* **2005**, *2*, 688-694
[32] Fanelli, F.; Fracassi, F.; d'Agostino, R. *Plasma Process. Polym.* **2007**, *4*, S430-S434
[33] Miskiewicz, S. J.; Arnett, B. B.; Simon, G. E. *Clin. Chem*. **1973**, *19*, 253−257.
[34] Selinheimo E., NiEidhin D., Steffensen C., Nielsen J., Lomascolo A., Halaouli S., Record E., O'Beirne D., Buchert J., Kruus K. *J Biotechnol.* **2007**, *130*, 471-80.